Published online 19 February 2018

Nucleic Acids Research, 2018, Vol. 46, No. 6 ***3075–3087***
doi: 10.1093/nar/gky108

eIF4A alleviates the translational repression mediated by classical secondary structures more than by G-quadruplexes

Joseph A. Waldron[1], Farheen Raza[1] and John Le Quesne[1,2,*]

[1]MRC Toxicology Unit, Leicester, UK and [2]Leicester Cancer Research Centre, University of Leicester, Leicester, UK

Received December 19, 2017; Revised February 02, 2018; Editorial Decision February 04, 2018; Accepted February 13, 2018

ABSTRACT

Increased activity of the mRNA helicase eIF4A drives cellular malignancy by reprogramming cellular translation, and eIF4A activity is the direct or indirect target of many emerging cancer therapeutics. The enriched presence of $(GGC)_4$ motifs, which have the potential to fold into two-layered G-quadruplexes, within the 5′UTRs of eIF4A-dependent mRNAs suggests that eIF4A is required for the unwinding of these structures within these eIF4A-controlled mRNAs. However, the existence of folded G-quadruplexes within cells remains controversial, and G-quadruplex folding is in direct competition with classical Watson–Crick based secondary structures. Using a combination of reverse transcription stalling assays and 7-deazaguanine incorporation experiments we find that $(GGC)_4$ motifs preferentially form classical secondary structures rather than G-quadruplexes in full-length mRNAs. Furthermore, using translation assays with the eIF4A inhibitor hippuristanol, both *in vitro* and in cells, we find that eIF4A activity alleviates translational repression of mRNAs with 5′UTR classical secondary structures significantly more than those with folded G-quadruplexes. This was particularly evident in experiments using a G-quadruplex stabilizing ligand, where shifting the structural equilibrium in favour of G-quadruplex formation diminishes eIF4A-dependency. This suggests that enrichment of $(GGC)_4$ motifs in the 5′UTRs of eIF4A-dependent mRNAs is due to the formation of stable hairpin structures rather than G-quadruplexes.

INTRODUCTION

Regulation of translation plays a major role in determining the final levels of proteins within the cell (1), and is finely controlled to ensure accurate composition of the proteome (2). In general, most regulation occurs at translation initiation, during which the eukaryotic initiation factor (eIF) complex eIF4F recruits the small ribosomal subunit to the 5′ end of the mRNA. This step is dependent on unwinding of secondary structures by eIF4F's effector subunit, the DEAD box RNA helicase eIF4A (3,4). The eIF4F complex is situated at the nexus of many mitogenic signalling pathways (5,6), where it exerts pervasive control over mRNA translation. These pathways are often hyperactivated in cancer cells, ensuring enhanced levels of translation, which is essential for their continued growth and survival (5–8). Increased eIF4A activity is a common feature of malignancy (9), often leading to drug resistance (10–12), and has become an attractive target for cancer therapeutics, with eIF4A-specific inhibitors showing very promising antineoplastic results in mouse models of the disease (13–15).

To gain an in-depth mechanistic understanding of why eIF4F activity is critical for driving malignancy, several groups, including our own, have carried out either polysome profiling or ribosome footprinting after eIF4A inhibition (9,13,16). Crucially, all three studies showed that the requirement for eIF4A activity was not equal among all mRNAs and that those mRNAs most dependent on eIF4A for their translation were enriched for transcripts encoding a range of oncogenic proteins such as CDC25B, c-MYC and cyclin D1 (9,13,16). These eIF4A-dependent mRNAs also had longer 5′UTRs, with increased propensity for secondary structures, suggesting a model in which cancer cells require higher levels of eIF4A activity in order to acquire an oncogenic translational program. Interestingly, two of these studies also reported that these 5′UTRs were enriched with a $(GGC)_4$ motif, that has the potential to fold into a G-quadruplex (9,13). This has been widely interpreted as evidence that these tertiary structures add an additional layer of regulation by conferring increased dependency on eIF4A activity to those mRNAs that possess potential quadruplex forming sequences within their 5′UTRs.

G-quadruplexes are stable structures formed from stacks of two or more G-tetrads (17). Each G-tetrad is composed of four guanine residues, where each guanine is bound to two others through Hoogsteen interactions. They have been

*To whom correspondence should be addressed. Tel: +44 116 252 5541; Email: jlq2@le.ac.uk

implicated in many aspects of RNA biology (18,19), including translation, where stable G-quadruplexes have been shown to inhibit cap-dependent translation (20–23). However, although it is accepted that they form in *in vitro* assays, whether or not they really fold in cells remains controversial (24), with evidence both in support (25–27) and against (28). Although bioinformatic searches for potential quadruplex sequences (PQSs) show these PQSs to be enriched in UTR regions (29), including the 5′UTRs of known oncogenic mRNAs (30) such as *BCL2* (31,32) and *NRAS* (33), it is clear that the presence of the sequence alone does not mean the G-quadruplex will be folded within a full length mRNA (24). Also, these searches historically looked for PQSs which would possess three G-tetrads and a loop of seven nucleotides or less, whereas it is now clear that G-quadruplexes can form *in vitro* with just two layers of G-tetrads, with large internal loops, and with bulges within the G-tracts (24,34–39). The $(GGC)_4$ motif that we and others see enriched in the 5′UTRs of eIF4A dependent mRNAs would fold into a G-quadruplex with just two layers of G-tetrads. Although biophysical techniques such as circular dichroism (CD) and ultraviolet (UV) melting curves are commonly used to demonstrate quadruplex folding for certain sequences, these techniques use short oligonucleotides, and cannot distinguish between inter-molecular and intra-molecular G-quadruplexes (24). Furthermore in full-length mRNAs, G-quadruplex formation is in direct competition with alternative secondary structures, notably with classical Watson–Crick base-paired helices (24). Biophysical techniques alone, therefore, cannot be relied upon to prove that a G-quadruplex is able to form in full length mRNAs.

To fully understand the biological implications of eIF4A inhibition, or the potential value of directly targeting G-quadruplexes, we must determine the extent, if any, by which G-quadruplexes confer increased dependency on eIF4A activity for translation. To this end we have carried out translation assays for a wide range of reporter constructs with different G-quadruplex forming sequences, both *in vitro* and in cells with and without the eIF4A-specific small molecule inhibitor hippuristanol (40). In parallel, we used reverse transcription stalling assays (41) to detect quadruplex folding in full length mRNA, and further tested the effects of G-quadruplex folding modulations by the use of synthetic nucleotides in *cis*, and quadruplex-binding small molecules in *trans*.

MATERIALS AND METHODS

Cell culture

MCF7 cells were cultured in DMEM (ThermoFisher 41966) with 10% FCS. Cells were tested regularly for mycoplasma and were authenticated by Eurofins using PCR-single-locus-technology.

Cloning

Annealed oligos were cloned into the pGL3-promoter plasmid (Promega E1761) between the HindIII and NcoI restriction sites directly upstream of the Fluc open reading frame. *CDC25B*, *GNAS* and *GNA11* were cloned by GenScript due to their length and high GC content. 5′UTR sequences, directly downstream of the SV40 promotor are shown in Supplementary Table S1. All constructs were verified with bi-directional Sanger sequencing.

PCR

Template DNA for the *in vitro* transcription reactions was synthesized using PCR from the plasmids used for DNA transfections, in order to incorporate the T7 binding site and $(A)_{25}$ tail. HCV-pRL template was synthesized from the HCV-pRL plasmid, kindly donated by Martin Bushell's lab. Primer sequences are shown in Supplementary Table S2. Q5 High Fidelity DNA Polymerase (M0491S) was used as per manufacturer's instructions with the addition of 1X Q5 High GC Enhancer.

In vitro transcription

mRNAs used in Figures 1, 3–5 and Supplementary Figure S3 were transcribed using the mMessage mMachine Ultra kit (ThermoFisher AM1345) as per manufacturer's instructions. This kit uses the anti-reverse cap analogue (ARCA) to ensure the cap is in the correct orientation. mRNA was purified using the MEGAclear kit (ThermoFisher AM1908) and quantified by nanodrop. Integrity of RNA was checked by inspection on a native agarose gel.

mRNAs used in Supplementary Figure S1 and Figure 2 were transcribed using the TranscriptAid T7 High Yield Transcription Kit (ThermoFisher K0441) as per manufacturer's instructions. For Supplementary Figure S1, 7.5 mM ATP/CTP/UTP, 1.5 mM GTP and either 6 mM ARCA (NEB S1411S) or 6 mM G(5′)ppp(5′)A RNA Cap Structure Analog (NEB S1406S) was used whereas for Figure 2, 7.5 mM ATP/CTP/UTP, 6 mM ARCA (S1411S) and either 1.5 mM GTP or 1.5 mM 7-deazaguanine (TriLink N-1044) was used.

HCV-Rluc RNA was transcribed with the MEGAscript kit (ThermoFisher AM1333) and was not capped.

RNA for reverse transcription stalling experiments was transcribed using the MEGAscript kit. This RNA was the same as that mRNA used in translation assays, except without a 5′ cap.

In vitro translation assays

Cell free extracts were derived from MCF7 cells following the protocol described in (42). Large volumes of cells were grown to 70–80% confluency using Nunc EasyFill Cell Factories. Cells were collected using trypsin, followed by deactivation with twice the volume of media with 10% FCS and washed twice with room temp PBS. The cell pellet was then resuspended with an equal volume of ice cold hypotonic buffer (10 mM Hepes pH 7.5, 10 mM KOAc, 0.5 mM MgOAc, 5 mM DTT, 1× EDTA free proteinase inhibitors) and left to swell on ice for 1 h (cells were kept in solution with gentle flicking every 10 min). Cells were homogenized by forcing through a 27G needle using a 1 ml syringe 15 times and centrifuged at 12 000g in a micro centrifuge for 5 min at 4°C. Supernatant was aliquoted and stored at -80°C. Protein concentration was measured using Bradford reagent. Each biological replicate used a different batch of extracts using cells grown and lysed on different days.

in vitro translation assays were carried out with 120 fmol Fluc reporter mRNA (150ng) and 120 fmol HCV-Rluc RNA (50 ng) in 15 μl reactions for 1 h at 37°C. Each reaction contained 100 μg cell free extract (5 μl), 15 mM Hepes (pH 7.5), 25 μg/ml creatine phosphokinase, 7.5 mM creatine phosphate, 0.1 mM spermidine, 75 mM KOAc, 0.75 mM MgOAc, 20 U RNasein Ribonuclease Inhibitor (Promega N2111) and the relevant concentration of either hippuristanol (kind gift from Junichi Tanaka), pyridostatin (Cambridge Bioscience) or an equal volume of DMSO. All of the above ingredients were first titrated so that the reaction was optimal; in our hands adding exogenous amino acids was not necessary. After the reactions had finished they were placed on ice and Fluc and Rluc measurements were obtained using the Dual-Luciferase Reporter Assay System (Promega E1980) and the GloMax-96 Microplate Luminometer. 25 μl of both the LAR II and Stop & Glo reagent were added to 5 μl of each *in vitro* translation reaction in duplicate. Biological replicates were carried out on different days.

Cellular translation assays

0.5×10^5 MCF7 cells were seeded per well in 24-well plates 16 h prior to transfection with 450 ng pGL3-promotor plasmid (with the relevant 5′UTR sequence cloned upstream of the Fluc ORF) and 50ng pRL Renilla Luciferase Control SV40 plasmid (Promega E2231), using 1.5 μl Lipofectamine 2000 transfection reagent (ThermoFisher 11668019) in duplicate. Eight hours afterwards, media was replaced with fresh media containing hippuristanol (kind gift from Junichi Tanaka), silvestrol (MedChem Express HY-13251), pyridostatin (Cambridge Bioscience) or DMSO. Cells were lysed 16 h later with 100 μl passive lysis buffer and Fluc and Rluc measurements were obtained using the Dual-Luciferase Reporter Assay System (Promega E1980) and the GloMax-96 Microplate Luminometer. Twenty five microlitre of both the LAR II and Stop & Glo reagent were added to 5 μl of lysate in duplicate. Biological replicates were carried out on different days.

Normalizing Fluc and Rluc measurements

in vitro translation assays were normalized to HCV-Rluc. The translation of Rluc was eIF4A-independent, as it is under the control of the HCV internal ribosome entry site (IRES). Levels of Rluc increased with increasing concentrations of hippuristanol, most likely due to the competition with cellular mRNAs, as these extracts were not nuclease treated. In cells however, transfection with the HCV-pRL plasmid produced Rluc which was very sensitive to hippuristanol, presumably as the mRNA will be transcribed in the nucleus and will therefore be capped. We therefore used the pRL Renilla Luciferase Control SV40 plasmid, which produces Rluc with a 5′UTR of moderate length and structure, to normalize against in cells. This was also sensitive to hippuristanol but less so than the HCV-Ren plasmid. HCV-Rluc and Rluc measurements were first adjusted by normalizing to the average change with hippuristanol, silvestrol or pyridostatin (or both hippuristanol and pyridostatin) within each biological replicate. For example, if hippuristanol caused Rluc measurements to decrease by 50% on average, each individual Rluc measurement with hippuristanol was divided by 0.5. This means that the average Rluc measurement for all reporters was the same between each treatment (with or without drug). Fluc measurements were then normalized to these adjusted Rluc measurements. Individual Fluc and Rluc levels are plotted for each experiment in Supplementary Figures S7–13.

Reverse transcription stalling

Reverse transcription stalling assays were essentially carried out as in (41). 2.5 pmol RNA was mixed with 5 pmol 5′ Cy5 labelled Luc RT primer (Supplementary Table S2) in 10 mM Tris–HCl (pH 7.5) and 75 mM KCl/LiCl in 5 μl. This was heated at 95°C in a thermal cycler for 1 min before cooling to 35°C. 2 μl 5× buffer (100 mM Tris–HCl (pH 8.4), 187.5 mM KCl/LiCl, 2.5 mM dNTPs, 20 mM $MgCl_2$ and 5 mM DTT) was added along with the relevant concentration of pyridostatin/DMSO and nuclease free water to take the reaction to 9.5 μl. The reaction was incubated at 35°C for 5 min, before the temperature was increased to 55°C where the reaction was incubated for 21 min, with 0.5 μl SuperScript III reverse transcriptase (200 U/μl) (ThermoFisher 18080044) being added after 1 min. 1 μl NaOH (1 M) was then added to the reaction and incubated at 95°C to degrade the RNA. Samples were then mixed with an equal volume of 2× loading buffer (95% formamide, 20 mM Tris–HCl (pH 8), 20 mM EDTA, 0.025% bromophenol blue), heated at 95°C for 3 min and 3.5 μl was loaded onto a pre-run 6% denaturing polyacrylamide sequencing gel. Gel was run at 45 W for 1.5 h which kept the temperature at 50°C and the gel was imaged using a Typhoon FLA 9000. Ladder sequences were run alongside and were made exactly as above, except adding 2 mM ddCTP to the reaction (4:1 ratio over dCTP)

RNA structure predictions

Predicted RNA structure and minimum free energy was calculated using RNAfold (43). GQRS mapper was used to confirm the presence/absence of overlapping/non-overlapping potential G-quadruplex sequences within our reporter constructs (44).

RESULTS

Experimental design

To test whether eIF4A is required to unwind G-quadruplexes within 5′UTRs during translation initiation, we designed reporter constructs with either four $(GGC)_4$ motifs or four $(GGGC)_4$ motifs within the 5′UTRs of firefly luciferase (FLuc) constructs (Figure 1A). These motifs have the potential to form either two-layered (GQ2) or three-layered (GQ3) G-quadruplexes. These reporters were used in translation assays with and without the eIF4A-specific inhibitor hippuristanol, both *in vitro* and in cells. *In vitro* assays utilized an MCF7 derived cell-free translation system, as in (42), that reconstitutes the synergism between the 5′ cap and the poly(A) tail, and in which hippuristanol inhibits translation of capped but not A-capped mRNAs (Supplementary Figure S1). The *in*

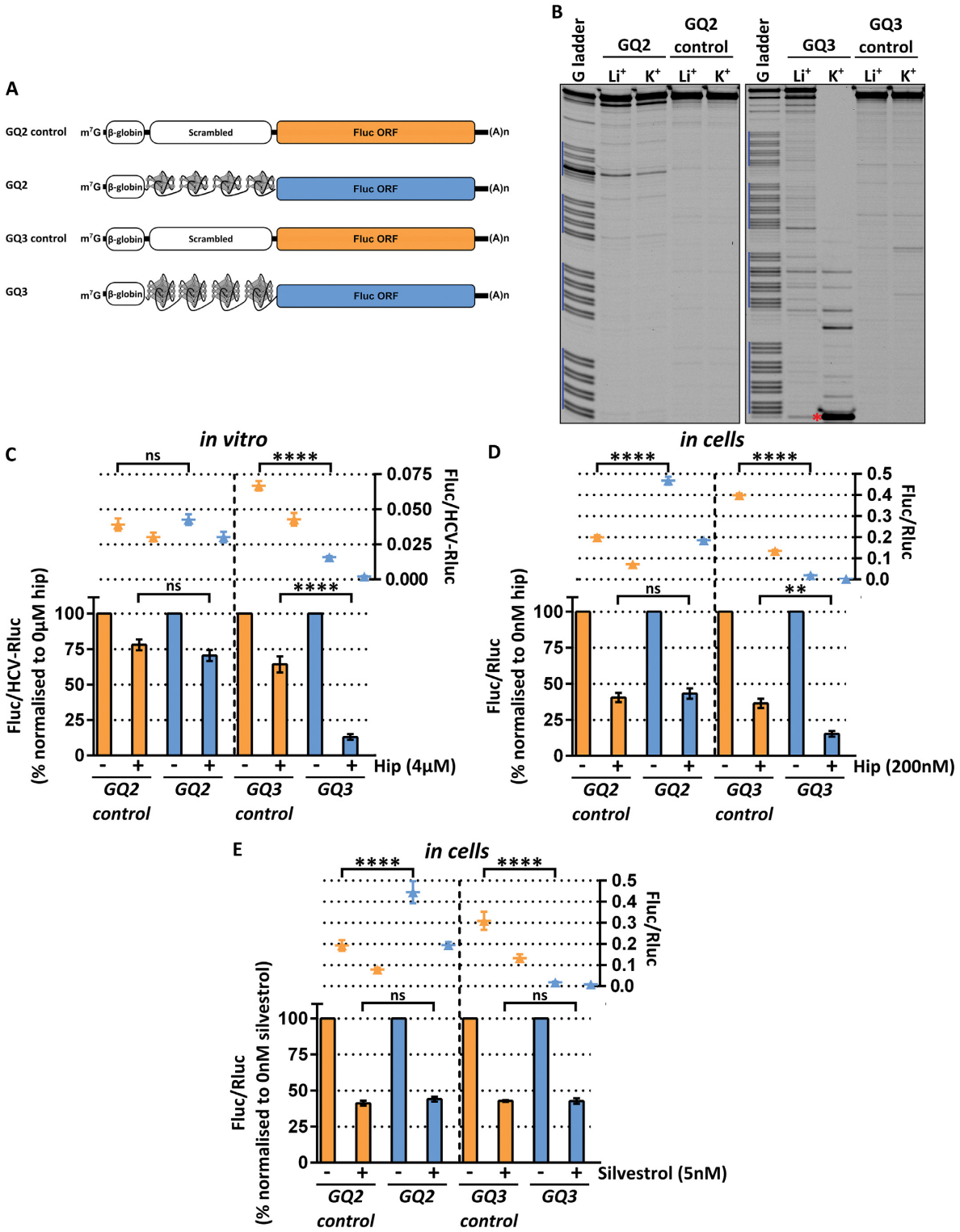

Figure 1. Three-layered but not two-layered G-quadruplexes cause eIF4A dependency. (**A**) Diagrammatic representation of the reporter constructs used in this figure. (**B**) Reverse transcription stalling assays using full length RNA shows K^+ dependent stalling (red star) one nucleotide before the G-quadruplex sequences (blue lines) in GQ3 but not GQ2 or either control. G-ladders were obtained from GQ2/3 RNA with Li^+ and the addition of ddCTP. (**C**) *in vitro* translation assays with and without 4 μM hippuristanol. Fluc was normalized to HCV-Rluc (right axis) and then normalized to 0 μM hippuristanol (left axis). $n = 4$ biological replicates. (**D** and **E**) Cellular translation assays with and without either 200 nM hippuristanol (D) or 5 nM silvestrol (E). Fluc was normalized to Rluc (right axis) and then normalized to 0 nM hippuristanol/silvestrol (left axis). $n = 3$ biological replicates. Error bars represent SEM. ns = not significant, $^{**}P < 0.01$ and $^{****}P < 0.0001$ using a repeated measures one-way ANOVA with Sidak's multiple comparisons test. Individual Fluc and Rluc measurements are presented in Supplementary Figure S7.

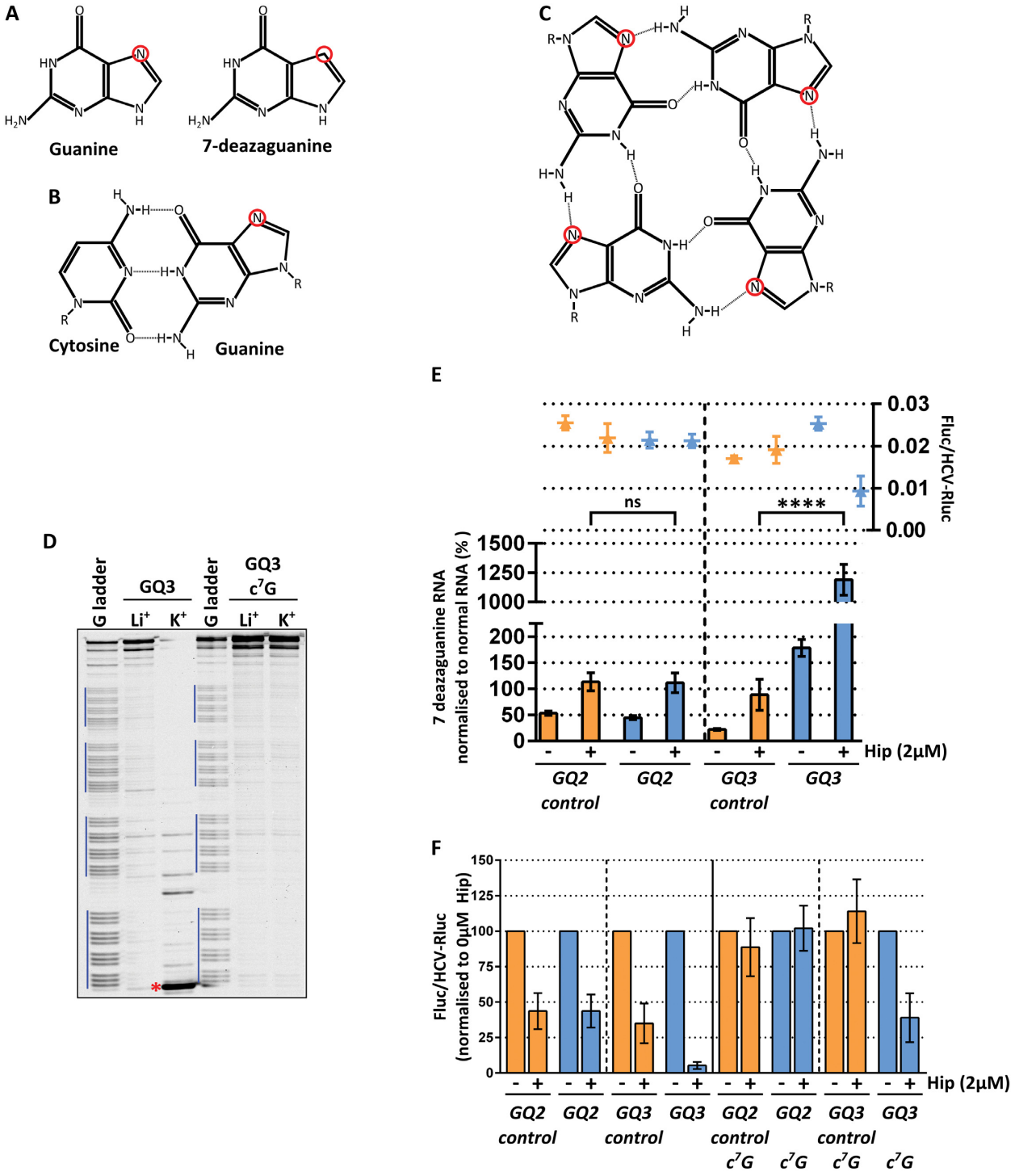

Figure 2. 7-deazaguanine de-represses GQ3 translation and eIF4A dependency. (**A**) Structure of guanine with the N^7 position circled in red and 7-deazaguanine with the C^7 position circled in red. (**B**) Structure of a Watson Crick G:C base pair. The N^7 position of guanine is circled in red. Hydrogen bonds are shown with dotted lines. (**C**) Structure of a G-tetrad, where each guanine is bound to two additional guanines through Hoogsteen base pairing. The N^7 position of guanine is circled in red. (**D**) Reverse transcription stalling assay shows that GQ3 RNA transcribed with 7-deazaguanine (c^7G) is unable to fold into G-quadruplexes, as evident from the absence of K^+ dependent stalling (red star) observed for GQ3. Each G-ladder was obtained from each RNA with Li^+ and the addition of ddCTP, demonstrating that the RNA sequence is the same. (**E** and **F**) *in vitro* translation assays with mRNA transcribed with 7-deazaguanine instead of guanine. For E, Fluc was normalized to HCV-Rluc (right axis) and then normalized to Fluc/HCV-Rluc values for the corresponding reporter transcribed with normal guanine (left axis). For F, each reporter was normalized to 0 μM hippuristanol. c^7G represents RNAs transcribed with 7-deazaguanine. $n = 3$ biological replicates. Error bars represent SEM. ns = not significant and $^{****}P < 0.0001$ using a repeated measures two-way ANOVA with Sidak's multiple comparisons test. Individual Fluc and Rluc measurements are presented in Supplementary Figure S8.

vitro translation assays have the advantage of a precisely known and quantified mRNA transcript, but otherwise relatively artificial conditions. By contrast, the cellular assays were performed by DNA transfection of MCF7 cells, ensuring nuclear origin and maturation of the mRNA, although the nature and quantity of the transcript is less controlled. These two complementary systems enable us to examine the importance of both exact mRNA sequence and 'natural' mRNA synthesis and biology. To determine the requirement of eIF4A activity for the translation of our reporters we measured the translational output of our reporters with and without hippuristanol. The sensitivity of our reporters to hippuristanol was used as a measure of eIF4A dependency. Reporters with 5′UTRs from previously determined eIF4A-dependent mRNAs (9) were more sensitive to hippuristanol than reporters with 5′UTRs from mRNAs showing the opposite tendency (Supplementary Figure S2), demonstrating that relative eIF4A dependency is measurable in this system.

It is known that eIF4A is required to unwind classical secondary structures both at the very 5′ end of the mRNA during ribosome recruitment, and further downstream during scanning (3). To test whether eIF4A is required to unwind G-quadruplexes during both steps, we placed the four potential G-quadruplex forming sequences either at the very 5′ end of the message (Supplementary Figure S3A) or downstream of the β-globin 5′UTR (Figure 1A), which is 50nt long with moderate predicted secondary structure. Control reporters were scrambled sequences with the same nucleotide composition but eliminated G-quadruplex forming potential.

Three-layered but not two-layered G-quadruplexes fold in full length mRNA reporters

To examine whether the sequences with G-quadruplex folding potential were folded in GQ2 and GQ3 reporters, we first carried out reverse transcription stalling assays as in (41). This technique relies on the fact that reverse transcriptases stall at folded G-quadruplexes and that G-quadruplex folding requires stabilization by a monovalent cation with a strong preference of K^+ over Li^+ (41). Using full length RNA we were able to detect GQ3 sequences folding *in vitro*, but we saw no evidence of GQ2 folding (Figure 1B). This was evident from the extra band (marked by red asterisk) observed for GQ3 with K^+ but not Li^+, one nucleotide before the G-quadruplex sequences, which is not seen for GQ2 or either controls.

Three-layered but not two-layered G-quadruplexes are inhibitory to translation and are more sensitive to eIF4A inhibition than controls

in vitro translation assays showed that the GQ2 reporter was translated at roughly the same levels as control and was no more sensitive to hippuristanol, yet GQ3 was clearly translationally repressed and significantly more sensitive to hippuristanol than control (Figure 1C). This was mirrored in the results from the cellular translation assays except that the GQ2 reporter was surprisingly translated higher than control, but its sensitivity to hippuristanol was not significantly different (Figure 1D). The increased sensitivity to hippuristanol observed for GQ3 but not GQ2 was also observed for the reporters with quadruplex sequences placed close to the 5′ end of the message both *in vitro* (Supplementary Figure S3B) and in cells (Supplementary Figure S3C).

Taken together, these data show that sequences that have the potential to fold into three-layered G-quadruplexes readily fold in 5′UTRs of full length mRNA and this causes translational repression with increased levels of eIF4A activity required for both ribosome recruitment and scanning. Meanwhile, two-layered G-quadruplexes were not seen to fold in the reverse transcription stalling assay, showed no increased sensitivity to hippuristanol compared to control, and actually yielded more protein than control in cells. This finding is in contrast with that of Wolfe *et al.* who found that in KOPT-K1 cells a GQ2 reporter was significantly more sensitive to the eIF4A inhibitor silvestrol compared to control (13). To test if these differing findings were due to the known different properties of different eIF4A inhibitors (45), we tested the sensitivity of our reporters to silvestrol in cells. Interestingly, neither GQ2 nor GQ3 were more sensitive to silvestrol than their controls (Figure 1E and Supplementary Figure S4). This provides further evidence that hippuristanol and silvestrol inhibit eIF4A activity through distinct mechanisms and suggests that the repertoire of mRNAs affected by such inhibition may be quite distinct. Hippuristanol is known to lock eIF4A in a closed conformation, unbound to RNA (40), thereby generating a loss of eIF4A function, whereas inhibitors of the rocaglate family, to which silvestrol belongs, act in a gain-of-function manner by increasing eIF4A's ability to 'clamp' upon polypurine rich sequences (46). Therefore, further experiments were carried out only with hippuristanol, to isolate the helicase function of eIF4A.

Ablation of G-quadruplex formation with 7-deazaguanine provides further evidence that three-layered but not two layered G-quadruplexes can fold and cause translational repression and eIF4A dependency

To ensure the reduced translational repression and increased eIF4A dependency of the GQ3 reporter was directly due to folded G-quadruplexes and not additional properties of the sequence, we made use of RNA transcribed with 7-deazaguanine (c^7G), which is identical to guanine except for a carbon atom instead of nitrogen at position 7 (Figure 2A). This N7 position is not involved in canonical Watson–Crick G:C base pairing (Figure 2B) but is essential for Hoogsteen base pairing between guanines within G-tetrads (Figure 2C). Replacing guanine with 7-deazaguanine in the *in vitro* transcription reaction therefore produces RNA capable of forming classical secondary structures but unable to fold into G-quadruplexes (47).

We first demonstrated that RNA transcribed with 7-deazaguanine cannot form G-quadruplexes, despite possessing the same nucleotide sequence, using reverse transcription stalling assays (Figure 2D). Interestingly mRNA transcribed with 7-deazaguanine was quite efficiently translated *in vitro*, showing that the N7 position is not vital to mRNA decoding. Levels of translation were reduced compared to normal RNA for the control reporters and GQ2, but almost 2-fold higher for GQ3 (Figure 2E, left axis). This

is further strong evidence that inhibitory G-quadruplex structures form in GQ3 but not in GQ2. We next sought to assess the impact that ablating G-quadruplexes had on eIF4A dependency. Although all four constructs were less sensitive to hippuristanol when transcribed with 7-deazaguanine, and GQ3 is still the most sensitive to hippuristanol (Figure 2F), the relative levels of translation from the 7-deazaguanine reporters compared to the normal RNA reporters was still much higher for GQ3 in the presence of hippuristanol (Figure 2E, left axis). Furthermore, the alleviation of G-quadruplex mediated repression for GQ3 is greater under conditions of eIF4A inhibition (Figure 2E, left axis), providing direct evidence that eIF4A activity is able to overcome the inhibitory effects of G-quadruplex formation on translation when folded.

$(GGA)_4$ sequences more readily fold into two-layered G-quadruplexes compared with $(GGC)_4$ sequences, yet are less sensitive to eIF4A inhibition

These findings are in conflict with the *in vivo* biochemical screens which specifically identified $(GGC)_4$ but not $(GGGC)_4$ motifs as being enriched in eIF4A-dependent 5′UTRs. One explanation, which is supported by the reverse transcription stalling assays, is that the $(GGC)_4$ motifs are not folding into G-quadruplexes in our synthetic reporters due to competing Watson–Crick interactions. To increase the likelihood for GQ2 folding we designed several more reporters in which the G-quadruplex sequences were placed in a $(CAA)_n$ background (Figure 3A), to minimize the amount of competing Watson–Crick interactions. As CAA repeats have previously been shown to be single stranded (48), this would also eliminate any secondary structures within the rest of the 5′UTR, allowing us to more directly compare the effects of the different quadruplex sequences on translation and eIF4A-dependency. We also wanted to investigate whether the identity of the nucleotide within the loop of the quadruplex is important for either quadruplex folding and/or conferring eIF4A-dependency, as the $(GGC)_4$ motif previously identified suggests this needs to be a cytosine to confer eIF4A-dependency. So that we could more directly compare the effects on translation and eIF4A-dependency between G-quadruplexes and hairpins we also designed hairpin constructs matched in length.

Alternative predicted structures and the predicted minimum free energy of each 5′UTR were generated using RNAfold (43), either favouring or preventing G-quadruplex formation (Supplementary Figure S5). Our control (C2) is predicted to be almost completely single stranded (Supplementary Figure S5A). GGCx1 is different by just one nucleotide and has the potential to form a two-layered G-quadruplex with C loops (Supplementary Figure S5B), but if this does not fold, the 5′UTR would also be almost entirely single stranded (Supplementary Figure S5C). GGAx1 is the same as GGCx1 except all the C loops have been replaced by A (Supplementary Figure S5D and E). GGCx2 and GGAx2 have the potential to form two two-layered G-quadruplexes (Supplementary Figure S5F and H). However, if these do not form, GGCx2 could form a modest hairpin structure with a predicted ΔG of -19.3kcal/mol (Supplementary Figure S5G), whereas GGAx2 would be mostly single stranded with a predicted ΔG of –1.1 kcal/mol (Supplementary Figure S5I). GQHP2 is the same as GGCx2, except that the second $(GGC)_4$ has been replaced with a $(CCG)_4$ motif. This means it could either form one, two-layered G-quadruplex (Supplementary Figure S5J) or a very stable hairpin structure of twelve G:C base pairs (Supplementary Figure S5K). HP2 has the potential to form the same hairpin structure as GQHP2, but with the first G:C base pair switched, eliminating any classical G-quadruplex potential (Supplementary Figure S5L).

Reverse transcription stalling assays show modest K^+ dependent stalling events with GGAx1 and more significant stalling with GGAx2 but none with either GGCx1 or GGCx2 (Figure 3B). This suggests that the cytosines in the predicted loop positions are preventing G-quadruplex folding, probably through competing Watson–Crick base pairing. The greatly increased stalling with GGAx2 compared to GGAx1 most likely reflects the fact that, although there are only two non-overlapping G-quadruplex-forming sequences in GGAx2, there are seventy potential overlapping G-quadruplex-forming sequences. These overlapping sequences could form G-quadruplexes from non-adjacent G-doublets, resulting in longer internal loops. This is supported by the presence of the higher band which represents stalling at one of these overlapping G-quadruplexes. The stalling events observed with GQHP2 and HP2 represent classical hairpin structures as they are not dependent on K^+.

The results obtained from the translation assays were different when carried out *in vitro* (Figure 3C) and in cells (Figure 3D). *in vitro*, GQHP2 and HP2 were translationally repressed and were the most sensitive to hippuristanol compared with all the two-layered G-quadruplex reporter constructs and control. This suggests that hairpins are more inhibitory to translation than two-layered G-quadruplexes due to a higher dependence on eIF4A activity. In support of this, GGCx2 was significantly more sensitive to hippuristanol than control but GGAx2 was not (Figure 3C), despite our RT stalling assays showing that GGAx2 is more likely to fold into a quadruplex than GGCx2 (Figure 3B), which likely adopts a hairpin structure (Supplementary Figure S5G). Interestingly, GGAx1 and GGAx2, which both form folded G-quadruplexes, were translated at higher levels than C2, GGCx1 and GGCx2 which do not. This suggests that folded two-layered G-quadruplexes are less inhibitory to translation than even modest secondary structures.

In cells, GQHP2 and HP2 were again translationally repressed but only GQHP2 was more sensitive to hippuristanol than control. Also, GGCx2 and GGAx2 were translated at higher levels than C2 but were not more sensitive to hippuristanol. The difference between results obtained *in vitro* and in cells is likely explained by the different methods of transcription for these mRNA reporters. Whereas the *in vitro* assays use *in vitro* transcribed RNA, where we can be sure that transcription starts at the guanine of the GAA-CAA, just upstream of the quadruplex sequence, transcription of the reporters in cells is under the control of the SV40 promoter which introduces upstream sequences. There are three possible transcription start sites for mRNAs derived from the SV40 promoter (49) and the sequences from all three sites are predicted to fold into stable secondary struc-

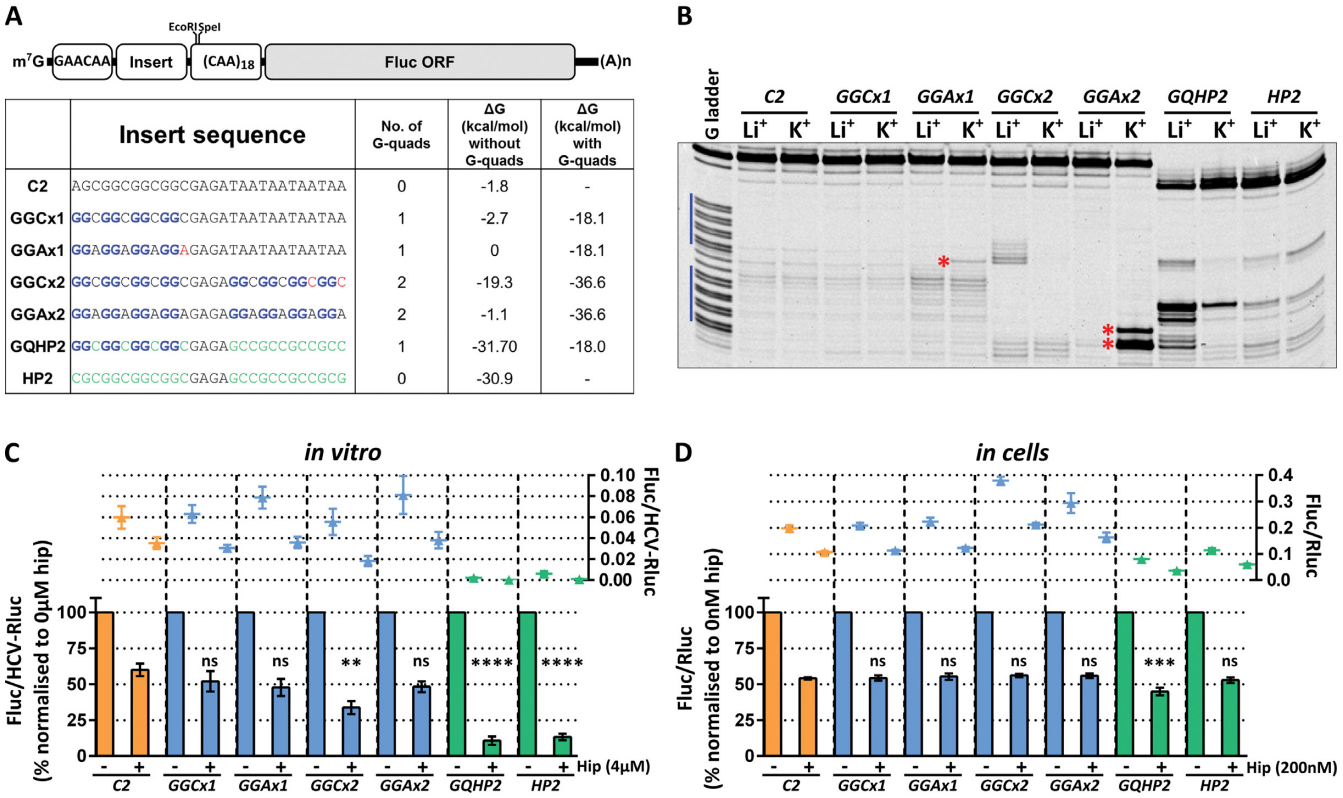

	Insert sequence	No. of G-quads	ΔG (kcal/mol) without G-quads	ΔG (kcal/mol) with G-quads
C2	AGCGGCGGCGGCGAGATAATAATAATAA	0	-1.8	-
GGCx1	GGCGGCGGCGGCGAGATAATAATAATAA	1	-2.7	-18.1
GGAx1	GGAGGAGGAGGAGATAATAATAATAA	1	0	-18.1
GGCx2	GGCGGCGGCGGCGAGAGGCGGCGGCGGC	2	-19.3	-36.6
GGAx2	GGAGGAGGAGGAGAGAGGAGGAGGAGGA	2	-1.1	-36.6
GQHP2	GGCGGCGGCGGCGAGAGCCGCCGCCGCC	1	-31.70	-18.0
HP2	CGCGGCGGCGGCGAGAGCCGCCGCCGCG	0	-30.9	-

Figure 3. $(GGA)_4$ but not $(GGC)_4$ sequences fold into G-quadruplexes but $(GGC)_4$ sequences confer more eIF4A dependency for translation. (**A**) Diagrammatic representation of the seven reporter constructs used in this figure. Guanines which can form G-quadruplexes are in bold and blue. Nucleotides in red correspond to the K^+ dependent stalling events marked by red asterisks in (B). Green nucleotides mark the stems of the hairpins in the two hairpin constructs. Predicted ΔG values are shown with and without quadruplex folding using RNAfold (43). (**B**) Reverse transcription stalling assays using full length RNA shows K^+ dependent stalling (red asterisk) one nucleotide before the G-quadruplex sequences (blue lines) in GGAx1 and GGAx2. G-ladder was made with GGCx2 RNA with Li^+ and the addition of ddCTP. (**C**) *in vitro* translation assays with and without 4 μM hippuristanol. Fluc was normalized to HCV-Rluc (right axis) and then normalized to 0 μM hippuristanol (left axis). (**D**) Cellular translation assays with and without 200 nM hippuristanol. Fluc was normalized to Rluc (right axis) and then normalized to 0 nM hippuristanol (left axis). $n = 3$ biological replicates. Error bars represent SEM. ns = not significant, $^{**}P < 0.01$, $^{***}P < 0.001$ and $^{****}P < 0.0001$ using a repeated measures one-way ANOVA comparing each value with C2, using Dunnet's multiple comparisons test. Individual Fluc and Rluc measurements are presented in Supplementary Figure S9.

tures (Supplementary Figure S6), thereby likely confounding the effects of our relatively small inserted elements, as well as potentially directly structurally interacting with them.

Pyridostatin stabilizes two-layered G-quadruplexes, which is inhibitory to translation

Overall, these findings suggest that within natural cellular 5′UTRs, two-layered G-quadruplexes are very unlikely to fold unless they are stabilized in some manner, for example by an RNA or G-quadruplex specific binding protein, or perhaps due to specific sequence context. We therefore decided to investigate the effect of quadruplex stabilization on translation and eIF4A-dependency, using the commercially available G-quadruplex stabilizing ligand pyridostatin (50).

In the presence of pyridostatin, we now observe additional reverse transcription stalling events one nucleotide before the G-quadruplex sequences in GQ2, GGCx1, GGCx2 and GQHP2 (Figure 4A and B). We also see increased stalling in GGAx1 and GGAx2 (Figure 4B). Crucially, this stalling is dependent on the N^7 moiety, as GQ2 RNA transcribed with 7-deazaguanine (c^7G) failed to stall the reverse transcriptase at these positions (Figure 4A), which demonstrates that the additional stalling bands are directly caused by quadruplex stabilization. Because, in the presence of K^+, three-layered G-quadruplexes are already folded and cause near-complete reverse transcriptase stalling, we needed to test the ability of pyridostatin to further stabilize these structures in the presence of Li^+. Under these conditions, pyridostatin does indeed stabilize three-layered G-quadruplexes, which is also N^7 dependent (Figure 4A).

The addition of pyridostatin to the *in vitro* translation assays inhibited translation of all reporters, but the levels of inhibition were significantly greater for reporters containing potential G-quadruplex forming sequences than controls (Figure 4C and D). GGAx2 was more sensitive to pyridostatin than GGCx2, further suggesting that $(GGA)_4$ sequences more easily fold into G-quadruplexes compared with $(GGC)_4$ sequences. Reporters with two potential non-overlapping quadruplex sequences were also more sensitive to pyridostatin than reporters with just one potential quadruplex sequence. Despite stabilizing G-quadruplex formation in GQHP2 in the reverse transcription stalling assay (Figure 4B), pyridostatin inhibited translation of GQHP2

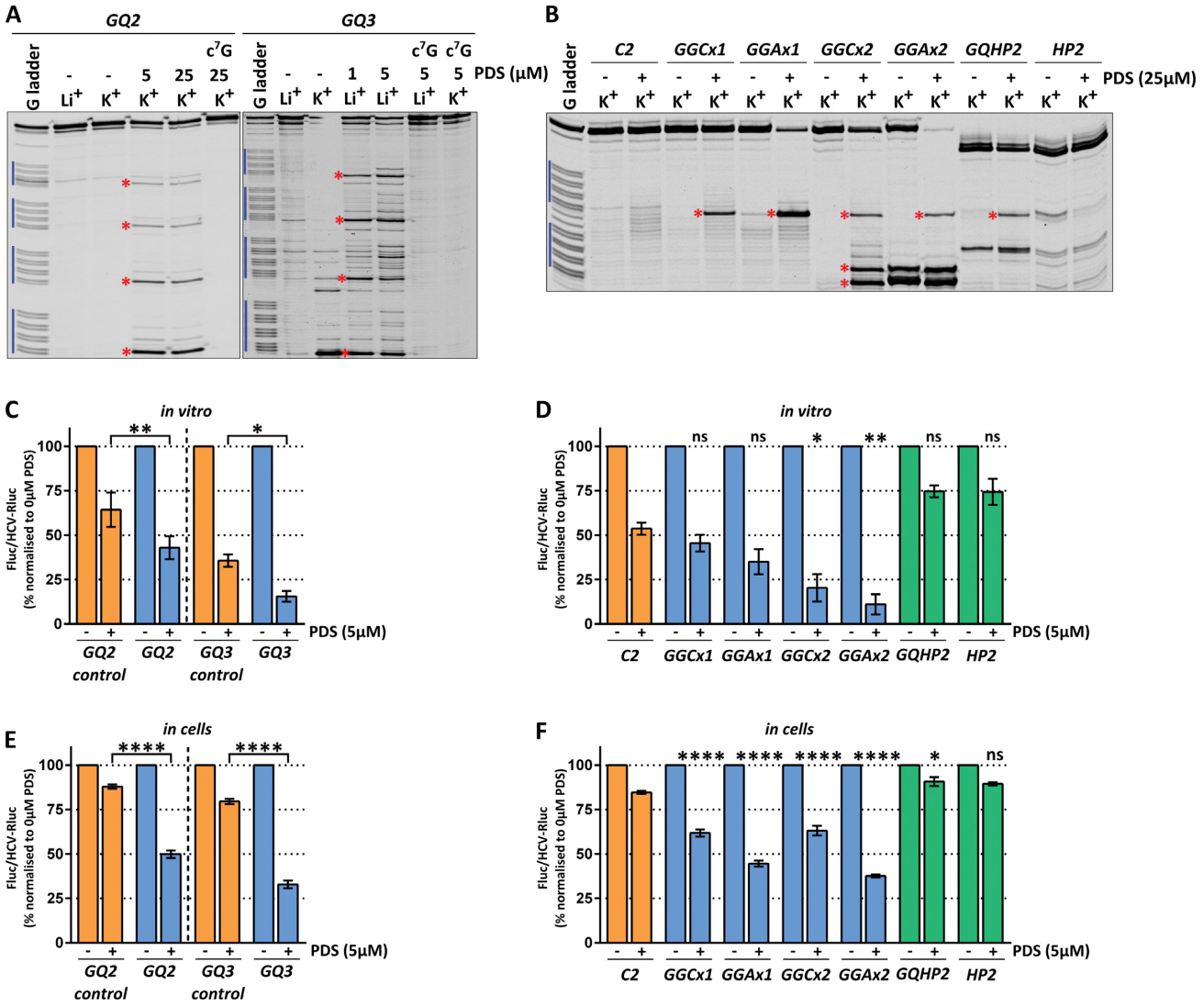

Figure 4. Pyridostatin stabilizes both two and three-layered G-quadruplexes, resulting in translational inhibition. (**A** and **B**) Reverse transcription stalling assays using full length RNA with and without pyridostatin. Stalling events (red asterisks) one nucleotide before the G-quadruplex sequences (blue lines) in the presence of pyridostatin indicates that this drug is able to stabilize these structures, which is not seen with RNA transcribed with 7-deazaguanine (c^7G). G-ladders are as used in Figures 1B and 3B. (**C** and **D**) *in vitro* translation assays with and without 5 μM pyridostatin. Fluc was normalized to HCV-Rluc and then to 0 μM pyridostatin. (**E** and **F**) Cellular translation assays with and without 5 μM pyridostatin. Fluc was normalized to Rluc and then to 0 μM pyridostatin. $n = 3$ biological replicates. Error bars represent SEM. ns = not significant, $^*P < 0.05$, $^{**}P < 0.01$ and $^{****}P < 0.0001$ using a repeated measures one-way ANOVA with Sidak's multiple comparisons test for (C and E) and Dunnet's multiple comparisons test for (D and F) comparing each reporter to C2 only. Individual Fluc and Rluc measurements are presented in Supplementary Figures S10 and S11.

less than C2 and to the same extent as HP2 which has no G-quadruplex potential, suggesting the stable hairpin structure in GQHP2 is able to outcompete G-quadruplex formation in the *in vitro* translation assay, even in the presence of pyridostatin.

The pyridostatin-induced reduction in translation from our controls suggests the possibility of non-canonical quadruplex formation, as has been shown previously (35). This could explain the faint increase in band intensity seen for C2 with pyridostatin (Figure 4B). The increased sensitivity to pyridostatin of C2 compared to GQHP2 and HP2 likely reflects the lack of any competing Watson–Crick interactions for C2, therefore increasing the chances of non-canonical quadruplex formation. The results obtained in cells matched those seen *in vitro*, except that reporters with two potential G-quadruplex sequences were no more sensitive to pyridostatin than reporters with just one potential G-quadruplex sequence (Figure 4E and F).

In summary, we find that in the presence of a G-quadruplex stabilizing ligand, two-layered G-quadruplexes do fold and do impede translation. How does this stabilization of G-quadruplexes influence eIF4A dependency? To investigate this, we carried out translation assays with and without pyridostatin, with and without hippuristanol for all our constructs both *in vitro* (Figure 5A and B) and in cells (Figure 5C and D).

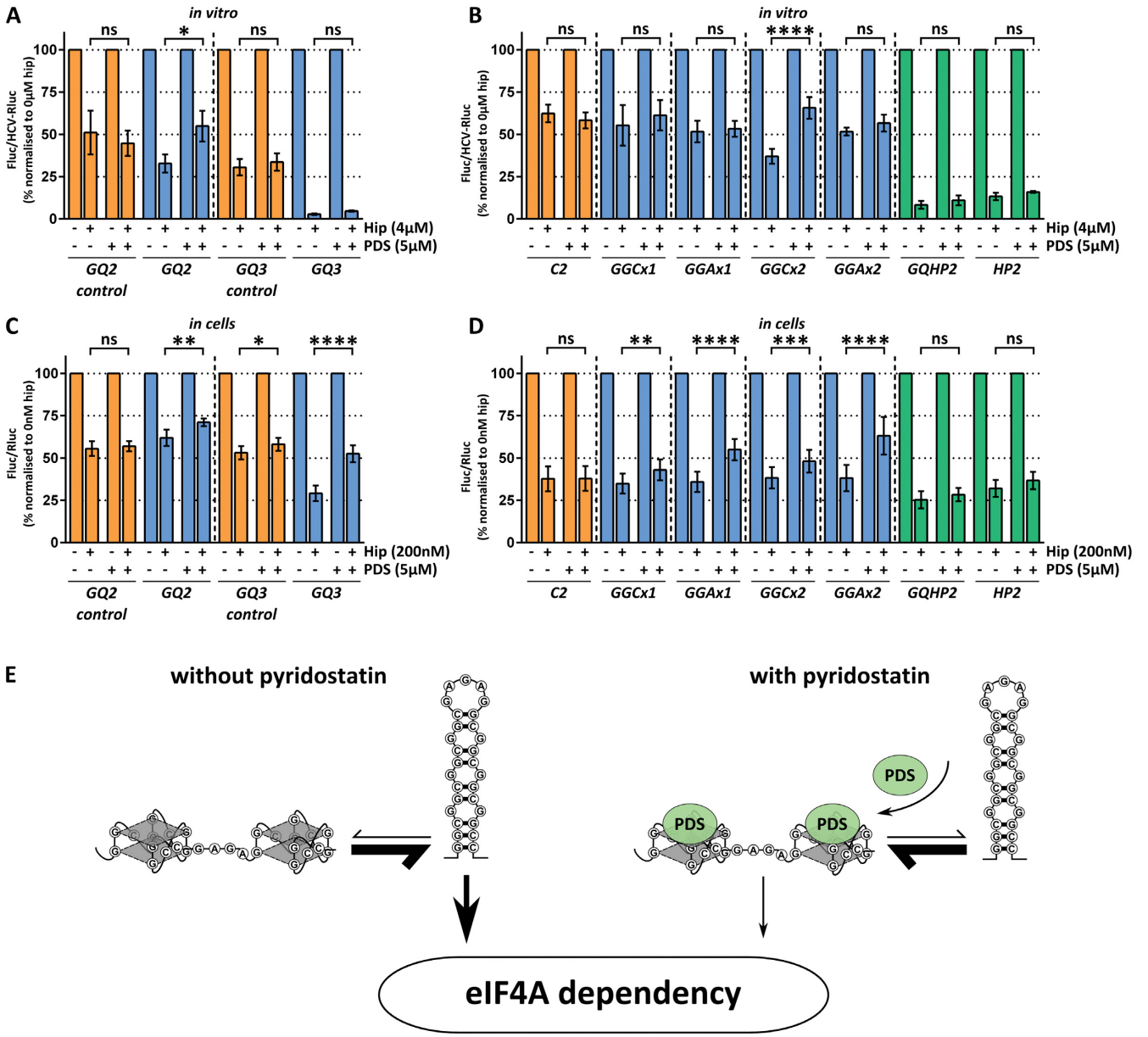

Figure 5. Reporters are more dependent on eIF4A activity when folded into hairpins than G-quadruplexes. (**A** and **B**) *in vitro* translation assays with and without 4 μM hippuristanol, with and without 5 μM pyridostatin. Fluc was normalized to HCV-Rluc and then to 0 μM hippuristanol with or without pyridostatin. (**C** and **D**) Cellular translation assays with and without 200 nM hippuristanol, with and without 5 μM pyridostatin. Fluc was normalized to Rluc and then to 0 nM hippuristanol with or without pyridostatin. $n = 3$ biological replicates. Error bars represent SEM. ns = not significant, $^{*}P < 0.05$, $^{**}P < 0.01$, $^{***}P < 0.001$ and $^{****}P < 0.0001$ using a repeated measures two-way ANOVA with Sidak's multiple comparison test. Individual Fluc and Rluc measurements are presented in Supplementary Figures S12 and S13. (**E**) Model summarizing our observations that classical Watson–Crick secondary structures confer increased dependency on eIF4A activity than G-quadruplexes. Under normal conditions, $(GGC)_4$ motifs prefer to fold into classical secondary structures rather than G-quadruplexes. mRNAs that possess these secondary structures within their 5′UTRs are more sensitive to eIF4A inhibition than if these sequences were folded into G-quadruplexes. This is supported by our observation that when the structural equilibrium is shifted in favour of G-quadruplexes with pyridostatin, the requirement for eIF4A activity is diminished.

$(GGC)_4$ sequences are more sensitive to eIF4A inhibition when folded into classical secondary structures than into G-quadruplexes

Strikingly, pyridostatin reduced the sensitivity to hippuristanol for GQ2 (Figure 5A) and GGCx2 (Figure 5B) but none of the other constructs *in vitro*. Therefore, the effect is restricted to those constructs that have the potential to fold into G-quadruplexes but only do so when stabilized by pyridostatin, such that when the equilibrium is shifted from classical Watson–Crick secondary structures towards G-quadruplexes the sensitivity to hippuristanol decreases (Figure 5E). This supports the hypothesis that canonical secondary structures confer increased dependency for eIF4A compared to G-quadruplexes, as the same sequence is more dependent on eIF4A when folded into a hairpin structure than when folded into a G-quadruplex. We can

rule out that this effect is simply due to pyridostatin binding the quadruplex which could disrupt eIF4A's ability to unwind the quadruplex, as the sensitivity to hippuristanol for GGAx2 is not affected by pyridostatin (Figure 5B).

In cells, we see reduced sensitivity to hippuristanol with pyridostatin for all our reporters with potential quadruplex sequences (Figure 5C and D). As described earlier these reporters will have extra 5′ sequence when transcribed in cells compared to *in vitro*, which could either interfere with quadruplex folding through competing Watson–Crick interactions or could fold into stable secondary structures which could dilute the effect that a downstream folded quadruplex has on translation. This data is therefore consistent with our hypothesis that the reduction in hippuristanol sensitivity/eIF4A dependency is due to a shift in structural equilibrium away from Watson–Crick structures and towards G-quadruplexes as these constructs now have the additional potential to fold into classical secondary structures in cells. In agreement with this, we saw a greater alleviation of hippuristanol sensitivity with pyridostatin for the GGA constructs compared to the GGC constructs (Figure 5D), due to these sequences more easily folding into G-quadruplexes. The fact that we see a strong alleviation in hippuristanol sensitivity with pyridostatin for GQ3 in cells (Figure 5C), but not *in vitro* (Figure 5A), suggests that the secondary structures introduced upstream by DNA transfection are more dependent on eIF4A activity for their unwinding than the three-layered G-quadruplexes.

DISCUSSION

This study aimed to dissect the role that G-quadruplex structures play in regulating translational control. *in vivo* biochemical screens from our lab (9) and others (13,16), had previously identified $(GGC)_4$ sequences as being enriched in the 5′UTRs of eIF4A-dependent mRNAs. It had previously been shown that these sequences can fold into G-quadruplexes using short oligonucleotides by biophysical techniques. It was expected that these sequences would also fold into G-quadruplexes in full-length mRNAs, and it is widely understood that this confers increased dependency on eIF4A for translation. However, not only do we find that $(GGC)_4$ sequences fail to fold into G-quadruplexes in reporter mRNAs, but the much less common, and generally non-enriched, $(GGA)_4$ sequences do fold into G-quadruplexes. Furthermore, $(GGC)_4$ elements are more dependent on eIF4A than $(GGA)_4$ elements, showing that the classical secondary structures formed by $(GGC)_4$ sequences dictate greater dependence upon eIF4A activity than the two-layered G-quadruplexes formed by $(GGA)_4$. In support of this, when we shifted the structural equilibrium of reporters from Watson–Crick secondary structures to G-quadruplexes, using a G-quadruplex stabilizing ligand, we observed a decrease in hippuristanol sensitivity/eIF4A dependency (Figure 5E).

Our data therefore suggest that the enrichment of $(GGC)_4$ motifs in the 5′UTRs of eIF4A-dependent mRNAs is a consequence of their ability to form classical Watson–Crick secondary structures rather than G-quadruplexes. It is possible that there is something innate about $(GGC)_4$-formed classical structures which demands higher levels of eIF4A activity compared with similar GC-rich sequences. Alternatively, given that $(GGC)_4$ sequences are the most common trinucleotide repeat within 5′UTRs (51), the enrichment of $(GGC)_4$ motifs may be a passenger phenomenon of general classical structure formation, given that we already know the requirement of eIF4A for translation is strongly associated with the degree of classical secondary structure within the 5′UTR (9,13,16,52).

Although we designed a wide range of reporters, we cannot rule out the possibility that the sequence/structural context of the G-quadruplex is key, and our system did not recapitulate this. Alternatively, a unique ability to switch between classical and G-quadruplex conformations innate to the $(GGC)_4$ motif may be biologically important in some way that we cannot as yet discern. Although three-layered G-quadruplexes do fold and strongly inhibit translation, and can be overcome by eIF4A activity, our data overwhelmingly support a model in which classical inhibitory Watson–Crick secondary structures are more susceptible to eIF4A inhibition. This explains why we see an enrichment of $(GGC)_4$ elements but not $(GGA)_4$ or $(GGU)_4$, or sequences that have the potential to fold into three-layered G-quadruplexes, enriched in the 5′UTRs of eIF4A dependent mRNAs.

Whatever the precise mechanisms at play, the central finding is that the ability to regulate mRNA translation by the alteration of eIF4A activity appears to be much more determined by classical Watson–Crick secondary structures rather than by G-quadruplexes. This has significant implications for the elucidation of this key axis in the control of both global and message-specific gene expression, and by extension the therapeutic targeting of this mechanism. Furthermore, even though $(GGC)_4$ elements rarely fold into G-quadruplexes in full length mRNAs, our findings that quadruplex folding can be stabilized for these sequences *in vivo*, and that this alleviates the sensitivity of these mRNAs to eIF4A inhibition, have interesting clinical implications for targeting translation via direct stabilization of G-quadruplexes.

SUPPLEMENTARY DATA

Supplementary Data are available at NAR Online.

ACKNOWLEDGEMENTS

We would like to thank Junichi Tanaka for kindly supplying us with hippuristanol, Ian Eperon and Cyril Dominguez for experimental ideas and insights and for critical reading of the manuscript, Tuija Poyry for experimental guidance and protocols, Ruth Spriggs for bioinformatic support, Manisha Patel for growing very large volumes of cells and also Anne Willis, Martin Bushell, and Julie Aspden for critical reading of the manuscript.

FUNDING

JLQ's MRC Toxicology Unit programme. Funding for open access charge: JLQ's MRC Toxicology Unit programme.
Conflict of interest statement. None declared.

REFERENCES

1. Schwanhausser,B., Busse,D., Li,N., Dittmar,G., Schuchhardt,J., Wolf,J., Chen,W. and Selbach,M. (2011) Global quantification of mammalian gene expression control. *Nature*, **473**, 337–342.
2. Livingstone,M., Atas,E., Meller,A. and Sonenberg,N. (2010) Mechanisms governing the control of mRNA translation. *Phys. Biol.*, **7**, 021001.
3. Jackson,R.J., Hellen,C.U. and Pestova,T.V. (2010) The mechanism of eukaryotic translation initiation and principles of its regulation. *Nat. Rev. Mol. Cell Biol.*, **11**, 113–127.
4. Hinnebusch,A.G. (2014) The scanning mechanism of eukaryotic translation initiation. *Annu. Rev. Biochem.*, **83**, 779–812.
5. Bhat,M., Robichaud,N., Hulea,L., Sonenberg,N., Pelletier,J. and Topisirovic,I. (2015) Targeting the translation machinery in cancer. *Nat. Rev. Drug Discov.*, **14**, 261–278.
6. Malka-Mahieu,H., Newman,M., Desaubry,L., Robert,C. and Vagner,S. (2017) Molecular pathways: the eIF4F translation initiation complex—new opportunities for cancer treatment. *Clin. Cancer Res.*, **23**, 21–25.
7. Chu,J. and Pelletier,J. (2014) Targeting the eIF4A RNA helicase as an anti-neoplastic approach. *Biochim. Biophys. Acta.*, **1849**, 781–791.
8. Raza,F., Waldron,J.A. and Quesne,J.L. (2015) Translational dysregulation in cancer: eIF4A isoforms and sequence determinants of eIF4A dependence. *Biochem. Soc. Trans.*, **43**, 1227–1233.
9. Modelska,A., Turro,E., Russell,R., Beaton,J., Sbarrato,T., Spriggs,K., Miller,J., Graf,S., Provenzano,E., Blows,F. *et al.* (2015) The malignant phenotype in breast cancer is driven by eIF4A1-mediated changes in the translational landscape. *Cell Death Dis.*, **6**, e1603.
10. Boussemart,L., Malka-Mahieu,H., Girault,I., Allard,D., Hemmingsson,O., Tomasic,G., Thomas,M., Basmadjian,C., Ribeiro,N., Thuaud,F. *et al.* (2014) eIF4F is a nexus of resistance to anti-BRAF and anti-MEK cancer therapies. *Nature*, **513**, 105–109.
11. Malka-Mahieu,H., Girault,I., Rubington,M., Leriche,M., Welsch,C., Kamsu-Kom,N., Zhao,Q., Desaubry,L., Vagner,S. and Robert,C. (2016) Synergistic effects of eIF4A and MEK inhibitors on proliferation of NRAS-mutant melanoma cell lines. *Cell Cycle*, **15**, 2405–2409.
12. Robert,F., Roman,W., Bramoulle,A., Fellmann,C., Roulston,A., Shustik,C., Porco,J.A. Jr, Shore,G.C., Sebag,M. and Pelletier,J. (2014) Translation initiation factor eIF4F modifies the dexamethasone response in multiple myeloma. *Proc. Natl. Acad. Sci. U.S.A.*, **111**, 13421–13426.
13. Wolfe,A.L., Singh,K., Zhong,Y., Drewe,P., Rajasekhar,V.K., Sanghvi,V.R., Mavrakis,K.J., Jiang,M., Roderick,J.E., Van der Meulen,J. *et al.* (2014) RNA G-quadruplexes cause eIF4A-dependent oncogene translation in cancer. *Nature*, **513**, 65–70.
14. Wiegering,A., Uthe,F.W., Jamieson,T., Ruoss,Y., Huttenrauch,M., Kuspert,M., Pfann,C., Nixon,C., Herold,S., Walz,S. *et al.* (2015) Targeting translation initiation bypasses signaling crosstalk mechanisms that maintain high MYC levels in colorectal cancer. *Cancer Discov.*, **5**, 768–781.
15. Tsumuraya,T., Ishikawa,C., Machijima,Y., Nakachi,S., Senba,M., Tanaka,J. and Mori,N. (2011) Effects of hippuristanol, an inhibitor of eIF4A, on adult T-cell leukemia. *Biochem. Pharmacol.*, **81**, 713–722.
16. Rubio,C.A., Weisburd,B., Holderfield,M., Arias,C., Fang,E., DeRisi,J.L. and Fanidi,A. (2014) Transcriptome-wide characterization of the eIF4A signature highlights plasticity in translation regulation. *Genome Biol.*, **15**, 476.
17. Kwok,C.K. and Merrick,C.J. (2017) G-Quadruplexes: prediction, characterization, and biological application. *Trends Biotechnol.*, **35**, 997–1013.
18. Cammas,A. and Millevoi,S. (2017) RNA G-quadruplexes: emerging mechanisms in disease. *Nucleic Acids Res.*, **45**, 1584–1595.
19. Millevoi,S., Moine,H. and Vagner,S. (2012) G-quadruplexes in RNA biology. *Wiley Interdiscip. Rev. RNA*, **3**, 495–507.
20. Halder,K., Wieland,M. and Hartig,J.S. (2009) Predictable suppression of gene expression by 5′-UTR-based RNA quadruplexes. *Nucleic Acids Res.*, **37**, 6811–6817.
21. Beaudoin,J.D. and Perreault,J.P. (2010) 5′-UTR G-quadruplex structures acting as translational repressors. *Nucleic Acids Res.*, **38**, 7022–7036.
22. Endoh,T. and Sugimoto,N. (2016) Mechanical insights into ribosomal progression overcoming RNA G-quadruplex from periodical translation suppression in cells. *Sci. Rep.*, **6**, 22719.
23. Kwok,C.K., Ding,Y., Shahid,S., Assmann,S.M. and Bevilacqua,P.C. (2015) A stable RNA G-quadruplex within the 5′-UTR of *Arabidopsis thaliana ATR* mRNA inhibits translation. *Biochem. J.*, **467**, 91–102.
24. Weldon,C., Eperon,I.C. and Dominguez,C. (2016) Do we know whether potential G-quadruplexes actually form in long functional RNA molecules? *Biochem. Soc. Trans.*, **44**, 1761–1768.
25. Biffi,G., Di Antonio,M., Tannahill,D. and Balasubramanian,S. (2014) Visualization and selective chemical targeting of RNA G-quadruplex structures in the cytoplasm of human cells. *Nat. Chem.*, **6**, 75–80.
26. Laguerre,A., Hukezalie,K., Winckler,P., Katranji,F., Chanteloup,G., Pirrotta,M., Perrier-Cornet,J.M., Wong,J.M. and Monchaud,D. (2015) Visualization of RNA-quadruplexes in live cells. *J. Am. Chem. Soc.*, **137**, 8521–8525.
27. Laguerre,A., Wong,J.M. and Monchaud,D. (2016) Direct visualization of both DNA and RNA quadruplexes in human cells via an uncommon spectroscopic method. *Sci. Rep.*, **6**, 32141.
28. Guo,J.U. and Bartel,D.P. (2016) RNA G-quadruplexes are globally unfolded in eukaryotic cells and depleted in bacteria. *Science*, **353**, aaf5371.
29. Huppert,J.L., Bugaut,A., Kumari,S. and Balasubramanian,S. (2008) G-quadruplexes: the beginning and end of UTRs. *Nucleic Acids Res.*, **36**, 6260–6268.
30. Zeraati,M., Moye,A.L., Wong,J.W., Perera,D., Cowley,M.J., Christ,D.U., Bryan,T.M. and Dinger,M.E. (2017) Cancer-associated noncoding mutations affect RNA G-quadruplex-mediated regulation of gene expression. *Sci. Rep.*, **7**, 708.
31. Shahid,R., Bugaut,A. and Balasubramanian,S. (2010) The *BCL-2* 5′ untranslated region contains an RNA G-quadruplex-forming motif that modulates protein expression. *Biochemistry*, **49**, 8300–8306.
32. Serikawa,T., Eberle,J. and Kurreck,J. (2017) Effects of genomic disruption of a guanine quadruplex in the 5′ UTR of the Bcl-2 mRNA in melanoma cells. *FEBS Lett.*, **591**, 3649–3659.
33. Kumari,S., Bugaut,A., Huppert,J.L. and Balasubramanian,S. (2007) An RNA G-quadruplex in the 5′ UTR of the *NRAS* proto-oncogene modulates translation. *Nat. Chem. Biol.*, **3**, 218–221.
34. Mukundan,V.T. and Phan,A.T. (2013) Bulges in G-quadruplexes: broadening the definition of G-quadruplex-forming sequences. *J. Am. Chem. Soc.*, **135**, 5017–5028.
35. Vlasenok,M., Varizhuk,A., Kaluzhny,D., Smirnov,I. and Pozmogova,G. (2017) Data on secondary structures and ligand interactions of G-rich oligonucleotides that defy the classical formula for G4 motifs. *Data Brief.*, **11**, 258–265.
36. Guedin,A., Gros,J., Alberti,P. and Mergny,J.L. (2010) How long is too long? Effects of loop size on G-quadruplex stability. *Nucleic Acids Res.*, **38**, 7858–7868.
37. Warner,K.D., Chen,M.C., Song,W., Strack,R.L., Thorn,A., Jaffrey,S.R. and Ferre-D'Amare,A.R. (2014) Structural basis for activity of highly efficient RNA mimics of green fluorescent protein. *Nat. Struct. Mol. Biol.*, **21**, 658–663.
38. Huang,H., Suslov,N.B., Li,N.S., Shelke,S.A., Evans,M.E., Koldobskaya,Y., Rice,P.A. and Piccirilli,J.A. (2014) A G-quadruplex-containing RNA activates fluorescence in a GFP-like fluorophore. *Nat. Chem. Biol.*, **10**, 686–691.
39. Kwok,C.K., Marsico,G., Sahakyan,A.B., Chambers,V.S. and Balasubramanian,S. (2016) rG4-seq reveals widespread formation of G-quadruplex structures in the human transcriptome. *Nat. Methods*, **13**, 841–844.
40. Cencic,R. and Pelletier,J. (2016) Hippuristanol—a potent steroid inhibitor of eukaryotic initiation factor 4A. *Translation (Austin)*, **4**, e1137381.
41. Kwok,C.K. and Balasubramanian,S. (2015) Targeted detection of G-quadruplexes in cellular RNAs. *Angew. Chem. Int. Ed. Engl.*, **54**, 6751–6754.
42. Rakotondrafara,A.M. and Hentze,M.W. (2011) An efficient factor-depleted mammalian *in vitro* translation system. *Nat. Protoc.*, **6**, 563–571.
43. Lorenz,R., Bernhart,S.H., Honer Zu Siederdissen,C., Tafer,H., Flamm,C., Stadler,P.F. and Hofacker,I.L. (2011) ViennaRNA Package 2.0. *Algorithms Mol. Biol.*, **6**, 26.

44. Kikin,O., D'Antonio,L. and Bagga,P.S. (2006) QGRS Mapper: a web-based server for predicting G-quadruplexes in nucleotide sequences. *Nucleic Acids Res.*, **34**, W676–W682.
45. Cencic,R., Galicia-Vazquez,G. and Pelletier,J. (2012) Inhibitors of translation targeting eukaryotic translation initiation factor 4A. *Methods Enzymol.*, **511**, 437–461.
46. Iwasaki,S., Floor,S.N. and Ingolia,N.T. (2016) Rocaglates convert DEAD-box protein eIF4A into a sequence-selective translational repressor. *Nature*, **534**, 558–561.
47. Weldon,C., Behm-Ansmant,I., Hurley,L.H., Burley,G.A., Branlant,C., Eperon,I.C. and Dominguez,C. (2016) Identification of G-quadruplexes in long functional RNAs using 7-deazaguanine RNA. *Nat. Chem. Biol.*, **13**, 18–20.
48. Pestova,T.V. and Kolupaeva,V.G. (2002) The roles of individual eukaryotic translation initiation factors in ribosomal scanning and initiation codon selection. *Genes Dev.*, **16**, 2906–2922.
49. Haegeman,G. and Fiers,W. (1980) Characterization of the 5′-terminal cap structures of early simian virus 40 mRNA. *J. Virol.*, **35**, 955–961.
50. Bugaut,A., Rodriguez,R., Kumari,S., Hsu,S.T. and Balasubramanian,S. (2010) Small molecule-mediated inhibition of translation by targeting a native RNA G-quadruplex. *Org. Biomol. Chem.*, **8**, 2771–2776.
51. Kozlowski,P., de Mezer,M. and Krzyzosiak,W.J. (2010) Trinucleotide repeats in human genome and exome. *Nucleic Acids Res.*, **38**, 4027–4039.
52. Svitkin,Y.V., Pause,A., Haghighat,A., Pyronnet,S., Witherell,G., Belsham,G.J. and Sonenberg,N. (2001) The requirement for eukaryotic initiation factor 4A (eIF4A) in translation is in direct proportion to the degree of mRNA 5′ secondary structure. *RNA*, **7**, 382–394.